PERGAMON

International Journal of Heat and Mass Transfer 41 (1998) 4009–4023

International Journal of HEAT and MASS TRANSFER

# Boiling stability characteristics of methanol flowing over a nonuniformly heated surface

W. W. Lin, J. C. Yang, D. J. Lee*

*Department of Chemical Engineering, National Taiwan University, Taipei, Taiwan, 106, Republic of China*

Received 1 March 1997

**Abstract**

The stability characteristics of methanol flow boiling over a nonuniformly heated surface has been investigated. An axial heat flux distribution corresponding to a neutral stability condition, at which nucleate and film boiling can coexist steadily, was identified under various system pressures, liquid subcooling and liquid flowrates. An increase (decrease) in the bottom heat flux under nucleate boiling mode would enhance (weaken) the relative stability of the film boiling mode. Furthermore, nucleate boiling would become more stable under increasing liquid subcooling. The dependence on system pressure is relatively weak. The 'equilibrium heat flux' is proven for the first time, to exist on an indirectly conductive heating surface, which can serve for direct comparison between stability characteristics among different boiling systems.


*Key words:* Flow boiling; Multi-mode boiling; Neutral stability; Pressure; Subcooling; System pressure

**Nomenclature**

$I$ integrand defined in eqn (1) [W K$^{-1}$ m$^{-2}$]
$P$ pressure [Pa]
$Q$ mass flowrate [kg m$^{-2}$ s$^{-1}$]
$q_b$ boiling heat flux [W m$^{-2}$]
$q_C$ equilibrium heat flux [W m$^{-2}$]
$q_F$ coexisting heat flux at point F [W m$^{-2}$]
$q_g$ bottom heat flux [W m$^{-2}$]
$q_N$ coexisting heat flux at point N [W m$^{-2}$]
$T$ temperature [K]
$T_F$ film boiling temperature [K]
$T_N$ nucleate boiling temperature [K]
$\Delta T_{sub}$ liquid subcooling [K]
$\Delta T_i$ temperature difference [K]
$V$ voltage [V].

## 1. Introduction

Boiling of different modes can coexist on the same heating element under certain conditions. In pool boiling with an electrically heated wire, steady state and unsteady state two-mode boiling (nucleate and film boiling) has been studied in detail [1–3]. With some others [4–7] important conclusions may be made as: (i) a unique 'equilibrium line' exists in each electrically heated wire boiling curve plot along which the nucleate and film boiling modes can coexist steadily; (ii) the intersections between the equilibrium line and the boiling curves have separated the nucleate and film boiling curves into stable and metastable regimes respectively; and (iii) an 'equal-area rule' (discussed later) can be employed in determining the location of the equilibrium line. A close analogy between the stability characteristics of a wire boiling system and that of classical vapor–liquid equilibrium (VLE) is noted.

Critical points, such as the critical heat flux (CHF) and minimum heat flux (MHF) points, denote the absolutely unstable points at which the system cannot tolerate infinitesimal disturbance. On the other hand, a heater under metastable nucleate boiling mode (i.e. the nucleate boiling curve below CHF and above the intersection between the equilibrium line and nucleate boiling curve) can tolerate a finite-magnitude disturbance (dry patch) to prevent burnout. However, when a large enough disturbance takes place, the heater would still transit into

* Corresponding author. Tel.: 00 886 2 362 5632; fax: 00 886 2 362 3040; e-mail: djlee@ccms.ntu.edu.tw

0017–9310/98 $19.00 
PII: 0017–9310(98)00107–0

film boiling. This is the so-called 'non-hydrodynamic' aspect for burnout [8, 9]; the nucleate boiling mode is thereby less stable than the film boiling mode in the metastable nucleate boiling regime. In contrast, if the heater is under stable nucleate boiling mode (i.e. the nucleate boiling curve below the intersection between the equilibrium line and nucleate boiling curve), no transit to film boiling would occur regardless of the magnitudes of the external disturbances, the boiling system can thereby tolerate infinitely large disturbances, and the nucleate boiling process is now more stable and is absolutely safe. Similar conclusions could be applied to the film boiling curve as well. When a heater under metastable film boiling regime (i.e. the film boiling curve below the intersection between the equilibrium line and film boiling curve) could transit to nucleate boiling when a large enough external disturbance (wet spot) has appeared on the boiling surface, and the film boiling mode is thus less stable than the nucleate boiling.

Identifying the points separating the metastable and stable boiling regimes is important in boiler design and operation. Kovalev [4], on the basis of wire boiling data, proposed the concept of so-called 'equilibrium heat flux', which divides the nucleate and film boiling curves into stable and metastable regimes, respectively. No experimental evidence supports that such an equilibrium heat flux exists for indirectly conduction heating boiling surface. Actually, except for the wire boiling systems, the information on the stability characteristics for the other more practical boiling systems (such as the usually employed conduction heated surface) is rarely reported in the literature.

Perhaps, Lin and Lee [10] have provided a first study about the relative stability between nucleate and film boiling modes on a conduction heated, flat plane heater under forced flow condition. They investigated the atmospheric multi-mode methanol flow boiling at a flow rate of 20 kg $m^{-2}$ $s^{-1}$ and a subcooling of 12 K. An axial (discrete) heat flux distribution with neutral stability, at which the nucleate and film boiling can coexist steadily (corresponds to the 'equilibrium line' for wire boiling system) is identified. Above such a distribution, the nucleate boiling mode is more stable; while below this the film boiling is more stable. The more stable nucleate boiling mode should be able to tolerate external disturbances to provide an absolutely safe nucleate boiling operation. The proposed nonuniformly heated boiling device is a convenient tool to investigate the relative stability among the nucleate and film boiling modes.

In this work, we provide more information about the relative stability between the nucleate and film boiling mode on a nonuniformly heated surface. The 'equilibrium heat flux' is identified for the first time for an indirect conduction heating surface.

## 2. Experimental

Figure 1(a) illustrates a schematic drawing of the experimental setup, which is a modified version of that employed in ref. [10]. The working liquid is methanol with purity of above 99%. The constant head maintained in the storage tank (1) and globe valve (7) has forced methanol to flow through the heat exchanger (3) and the flow meter (4) to the testing section (5). The receiving tank (8) is opened to an aspirator (11) through a condenser (10). Methanol in the receiving tank is then pumped back to the storage tank by a gear pump (9). The flow path through the storage tank, testing section and the receiving tank form the boiling loop. The boiling dynamics are recorded by a CCD camera (6).

Figure 1(b) shows the details of the testing section, consisting of an expanding section (11), a central flow chamber of dimension ($L \times W \times H$) $24 \times 8 \times 8$ $cm^3$ with front and rear view glasses (12), and a contracting section (13). The upper surface of the testing block matches the lower part of the central flow chamber exactly, permitting an undisturbed crossflow without generation of secondary flow above the heating surface. The fluid temperature is measured by a thermocouple.

Under the testing block are two (not three as employed in ref. [10]) independent heating blocks equipped with cartridge heaters, from which the joule heat can generate separately and transit to the top surface. The gap (width 10 mm) between these heating blocks is insulated to prevent direct heat conduction between them. Temperatures at 24 positions in the testing block are measured by thermocouples, whose readings are sent at a rate of 1 Hz to a data acquisition system (12) connected to a personal computer (13). Figure 1(c) shows the details of the heating assembly. In each heating block there are eight cartridge heaters, each of 157 W (220 V) capacity, giving out a maximum of 1336 W capacity in each block.

The testing block is made of pure copper, most of which (93% from the bottom) is divided into two separate parts with a gap of 5 mm between. Insulation is employed in these gaps to prevent heat conduction. Axial heat conduction is therefore permitted only in the top 7% (bridge) connection sections of thickness 2 mm. The joule heat from the bottom cartridge heaters can thereby transit vertically across most of the testing block to the bridge region, dissipate partially by surface boiling, and exchange the rest with the other block, if a temperature gradient exists between them.

The upper heating surface is a smooth surface of dimension 80 mm $\times$ 15 mm. The positions of the 24 thermocouples are also indicated in Fig. 1(c). The corresponding six axial positions above these thermocouples along the flow direction are referred to as B1 to B6, respectively. B1–B3 are heated by the cartridge heaters below the leading portion (denoted as portion L) of the heating surface; while B4–B6, the subsequent portion (denoted as portion S) are heated along the flow direction.

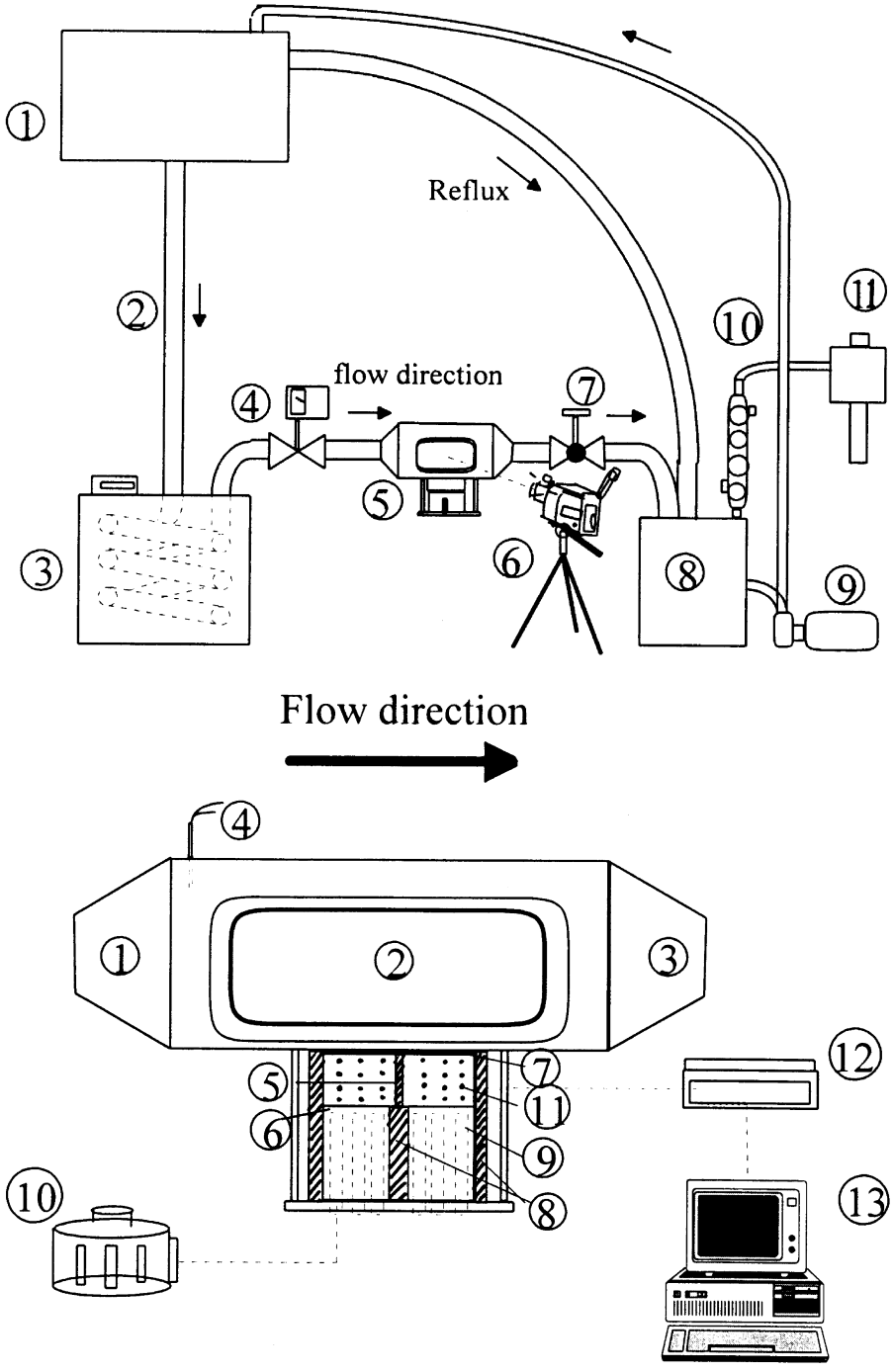


Fig. 1. (a) Schematics of boiling apparatus: (1) store tank, (2) connecting pipe, (3) heat exchanger, (4) flow meter, (5) testing section, (6) camera, (7) globe valve, (8) receiving tank, (9) gear pump, (10) condenser, (11) aspirator. (b) Schematics of testing block: (1) expanding section, (2) testing chamber, (3) contracting section, (4) thermocouple, (5) heating block, (6–8) insulation, (9) cartridge heaters, (10–11) thermocouples, (12) data acquisition system, (13) personal computer.

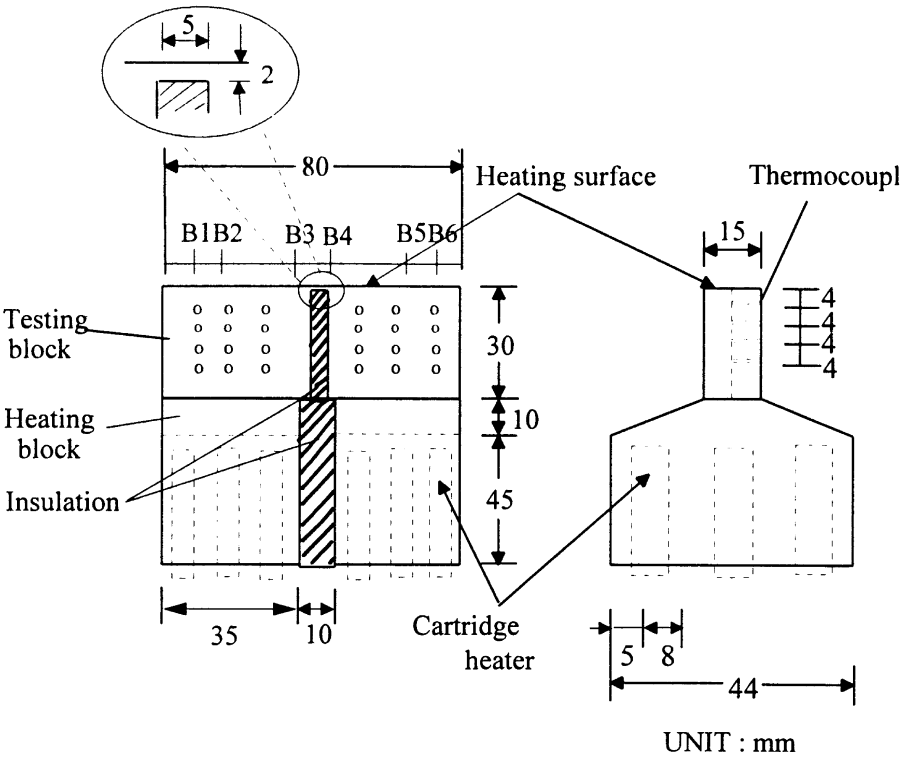


Fig. 1. (c) Schematics of heating assembly.

To prevent liquid leakage and the associated heat loss, a thin silicon rubber ring of thickness 2 mm is used as the sealing material between the bridge region of the testing block and the stainless steel flow chamber. This limits the time interval and the temperature level at which the film boiling can be sustained on the heating surface.

The system pressure and liquid temperature are adjusted by aspirator and heat exchanger. After reaching the steady state, all cartridge heaters are set at a voltage of $V_1$ to let all of the heating surface (B1–B6) enter a nucleate boiling mode (phase I). Then the voltage of the cartridge heaters in one of the bottom heating blocks (e.g. the portion L) is set at a high voltage of $V_2$ (phase II), which forces the corresponding top surface to enter film boiling. Once a visible film boiling has established on the boiling surface, the voltage of the bottom cartridge heaters is decreased from $V_2$ to $V_3$ to prevent burnout of the sealing silicon rubber (phase III). (Notably, the voltage for the other heating block is always kept at $V_1$). The high temperature under film boiling mode could cause a large axial heat conduction across the near-surface bridge connections to the other block.

The method of Kline and McClintock [11] has been employed to estimate the uncertainties in heat flux and temperature measurements. The uncertainty in thermocouple calibration is within 1 K in this study. The error in thermal conductivity data is estimated at not being higher than 2%. The maximum uncertainties thereby existing in the extrapolated heating surface temperature and the associated heat flux, which are estimated as $\pm 7$ and $\pm 11\%$, respectively. The mass flowrates exhibit an uncertainty of approximately $\pm 5\%$, while for fluid temperature measurement the uncertainty is $\pm 1$ K. The ripples in voltage outputs from the transformer are less than $\pm 2\%$.

## 3. Results and discussion

### 3.1. General

Figure 2 shows the time evolution of extrapolated, axial wall superheat temperature of a typical run under $P = 760$ mmHg, $\Delta T_{sub} = 0$ K, and $Q = 20$ kg m$^{-2}$ s$^{-1}$ with $V_1$, $V_2$, $V_3 = 80, 220, 60$ V, respectively. In this case, the subsequent section S is raised to film boiling mode. The time evolution of the boiling modes for B4, B5 and B6 are nucleate → film → nucleate; for B1, B2, the boiling is always in nucleate boiling; while for B3, nucleate → transition → nucleate. That is, the film boiling mode set up on the portion S fails to sustain but returns back to

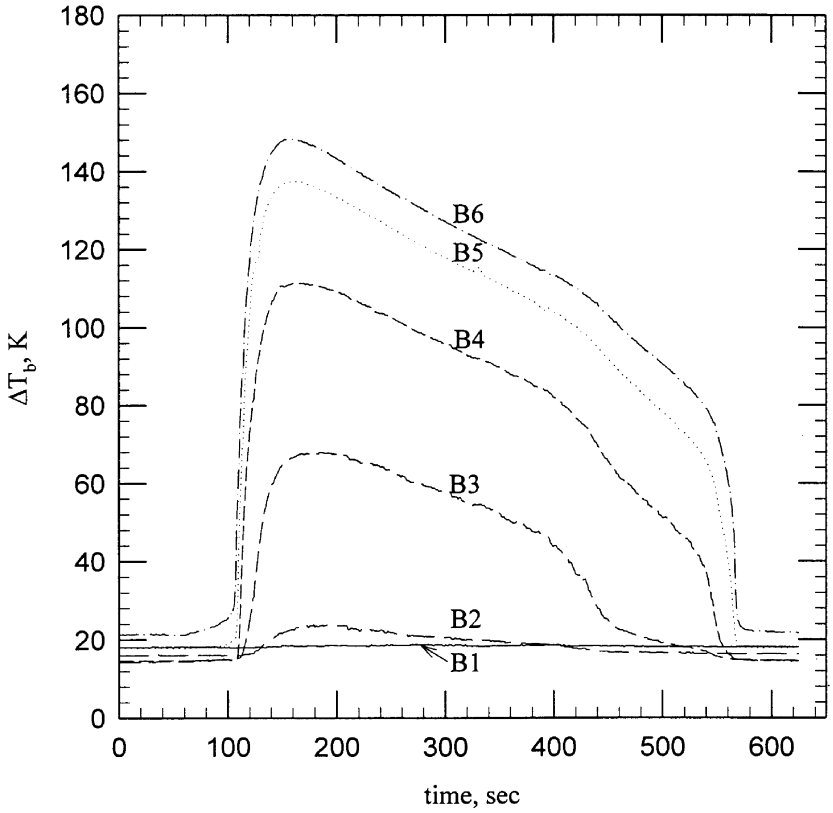


Fig. 2. Time evolution of extrapolated surface temperature data: $V_1$, $V_2$, $V_3$ = 80, 220, 60 V respectively; $P$ = 760 mmHg; $Q$ = 20 kg $m^{-2}\,s^{-1}$; $\Delta T_{sub}$ = 0 K.

the nucleate boiling mode via axial heat conduction with portion L.

Figure 3 shows the time evolution for an almost identical run but with a higher $V_3$ (80 V). A different pattern results. The modes for the whole heating surface have transited from nucleate to film boiling, following the sequence B6–B1. As a result, the film boiling mode established at B4–B6 is now stronger than the nucleate boiling mode originally existing at B1–B3. Since the temperatures have become too high (above 400°C), all cartridge heaters are cut off after 230 s. This is evidenced by the decreasing temperatures as observed in the final phase of the experiment.

Figure 4 depicts the evolution of surface temperature distribution for the above two cases. Figure 4(a) corresponds to the experimental sequence in Fig. 2, during which the temperature distribution approaches, but never attains to, the bold curve indexed as curve NF. Figure 4(b) reveals, on the other hand, an overshoot across the curve NF. As suggested in Lin and Lee [10], the curve NF is the coexisting curve of a neutral stability. Figure 5 illustrates the boiling phenomena observed close to the curve NF. Since $V_3$ in Fig. 4(a) is 60 V, and in Fig. 4(b), 80 V, a critical $V_3$ exists among them, which is approximately 70 V. If $V_3$ is set above this critical value, all states on the boiling surface will be attracted to the film boiling mode; if lower than this critical value, the final state is the nucleate boiling mode.

### 3.2. *Equal-area criterion*

Based on the heat conduction equation and the no-flux boundary conditions, the following equal-area criterion is used to interpret the multi-mode boiling data [3, 10, 12]:

$$I = \int_{T_N}^{T_F} (q_b - q_g)\,dT$$

$$\cong \sum_{i=1}^{5} 1/2((q_b(T_i) - q_{gi}) + (q_b(T_{i+1}) - q_{g,i+1}))\Delta T_i = 0, \quad (1)$$

where $T_F$ and $T_N$ are respectively the temperature under film and nucleate boiling, $q_b$ the boiling heat flux, and $q_g$, the bottom heat flux provided by indirect conduction heating, subscripts 1–6 denote positions B1 to B6 accordingly, and $\Delta T_i = T_{i+1} - T_i$. Along curve NF, the integrand is expected to be zero.

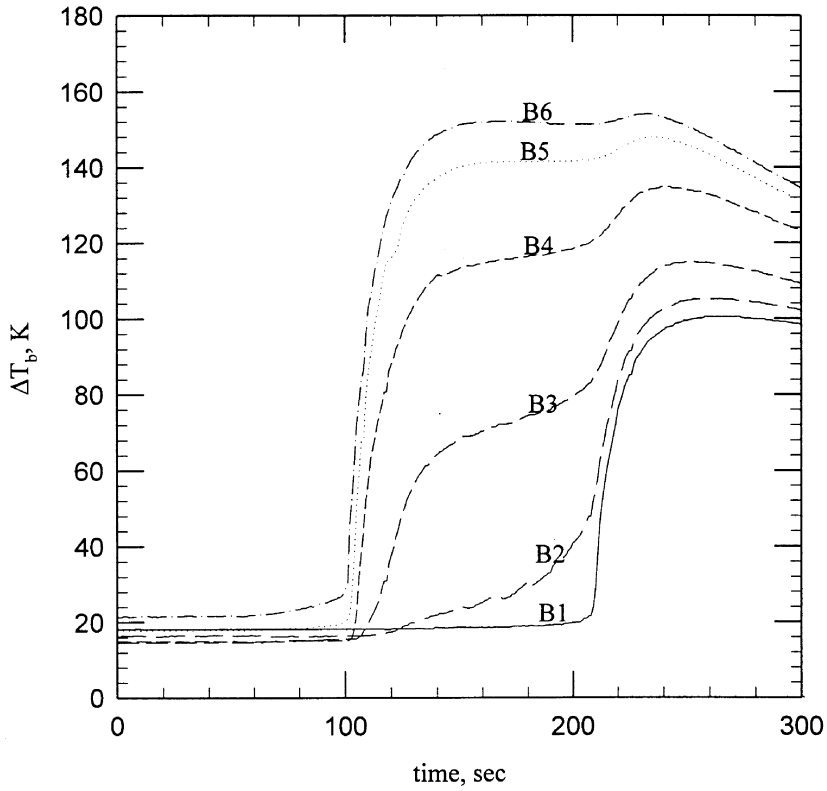


Fig. 3. Time evolution of extrapolated surface temperature data: $V_1$, $V_2$, $V_3$ = 80, 220, 80 V respectively; $P$ = 760 mmHg; $Q$ = 20 kg $m^{-2}$ $s^{-1}$; $\Delta T_{sub}$ = 0 K.

Figure 6 represents the NF curve and the corresponding boiling curves. (Note: (1) the true transition curve cannot be obtained directly from the present heat conduction-controlled apparatus [13], while the transition boiling curve is the connection between the CHF and MHF points on a plot in log–log scale for the first approximation; (2) the shape of NF curve varies according to the lateral heat conduction.) Notably, the areas between the boiling curve and the NF curve are similar, which supports the theory that the integrand in eqn (1) is zero along NF. Figure 7 illustrates the corresponding evolution paths of $I$ values for those depicted in Fig. 1(a) (squares) and in Fig. 4(b) (circles), with 'MB' representing the 'multi-mode boiling''. The approximation is rather rough as limited data points, only six are examined along the heating surface and the fuzziness of the location of true transition boiling curve, (a discussion on the average and true transition boiling curve can be found in [3]). When the whole surface is covered with only nucleate or film boiling, owing to almost no temperature gradient existing along the surface, the corresponding $I$ value is close to zero. The appearance of temperature and heat flux variation along the heater surface causes the $I$ value to become negative due to the rapid increase of surface temperature at B4–B6, and largely increasing thereby the area B in Fig. 6.

Evidently, a $V_{3critical}$ exists for a given heater/fluid/$V_1$ combination. As $V_3 < V_{3critical}$, $I$ is always negative, indicating a stronger boiling heat dissipation rather than generation, therefore a more stable nucleate boiling mode. When $V_3 > V_{3critical}$, the $I$ value will change sign from negative to positive, indicating a stronger heat generation, and thereby a more stable film boiling mode. At $V_3 = V_{3critical}$, the integrand $I$ is zero and a steady-state coexisting boiling results. We [10] propose also that, the surface heat flux vs wall superheat plot at $V_3 = V_{3critical}$ is an unstable steady-state; a small disturbance would push the state towards the stable nucleate or the stable film boiling state. An increase in $V_1$ or $V_3$ corresponds to increasing the bottom heat flux $q_g$ in eqn (1). A change in system pressure, flow rate or liquid subcooling results in changes of boiling heat flux $q_b$ and the associated wall superheat differences in eqn (1).

### 3.3. *Coexisting heat fluxes*

The bottom heat fluxes vary continuously in a test. In this study the 'coexisting heat fluxes' $q_N$ and $q_F$ are

respectively, at points N and F. Table 1 lists typical $q_N$ and $q_F$ data under atmospheric and subatmospheric pressure. Clearly from the data listed, an increase in $q_N$ will lead to a decrease in $q_F$, which is reasonable since nucleate boiling at higher bottom heat flux is less stable in nature. The comparisons between $Q = 12$ and $Q = 20$ kg m$^{-2}$ s$^{-1}$ reveal that the nucleate boiling mode becomes more stable under higher liquid mass flowrate. The lower $q_F$ for higher $\Delta T_{sub}$ indicates a more stable nucleate boiling mode under subcooled condition. These results are to be expected since a higher mass flowrate and/or a lower liquid temperature would raise the corresponding CHF and MHF points, and a more efficient film boiling curve. The $q_N$ and $q_F$ data under various system pressures and saturated condition show that, an increase in $q_N$ will result in a decrease in $q_F$, as well. However, at fixed $q_N$, a decrease in system pressure will, on the contrary, give a higher $q_F$, although the dependence is rather weak.

### 3.4. *Equilibrium heat flux*

The above-mentioned results reveal that the coexisting heat fluxes data, $q_N$ and $q_F$, are good indices addressing to the stability characteristics of boiling; while the equal-area criterion can be viewed as a basis for data interpretation. However, the present investigation suggests that the stability of nucleate and film boiling mode on a heating surface is relative, i.e. the locations of point N and F are dependent on each other. As the heat flux at point N (nucleate boiling mode) becomes higher, the corresponding NF curve shifts downwards accordingly. Actually, there exist infinitely many possible NF curves, and thereby equilibrium heat fluxes, for a given heater/boiling liquid combination that can fulfil the equal-area criterion. In practice, a uniform rather than a nonuniform heat flux distribution is more often employed. The 'equilibrium heat flux' proposed by Kovalev [4] is the quantity of concern.

Figure 8 plots one typical ($q_N$, $q_F$) set for $P = 760$ mmHg, $\Delta T_{sub} = 0$ K, and $Q = 20$ kg m$^{-2}$ s$^{-1}$. The intersection between the extrapolation for data set (closed symbols) and the 45° line gives a point where $q_N = q_F = q_C$, which is unique for this specific heater/liquid combination. On the boiling curve plot $q = q_C$ indicates a horizontal line, which is the 'equilibrium heat flux' proposed by Kovalev [4]. This is for the first time

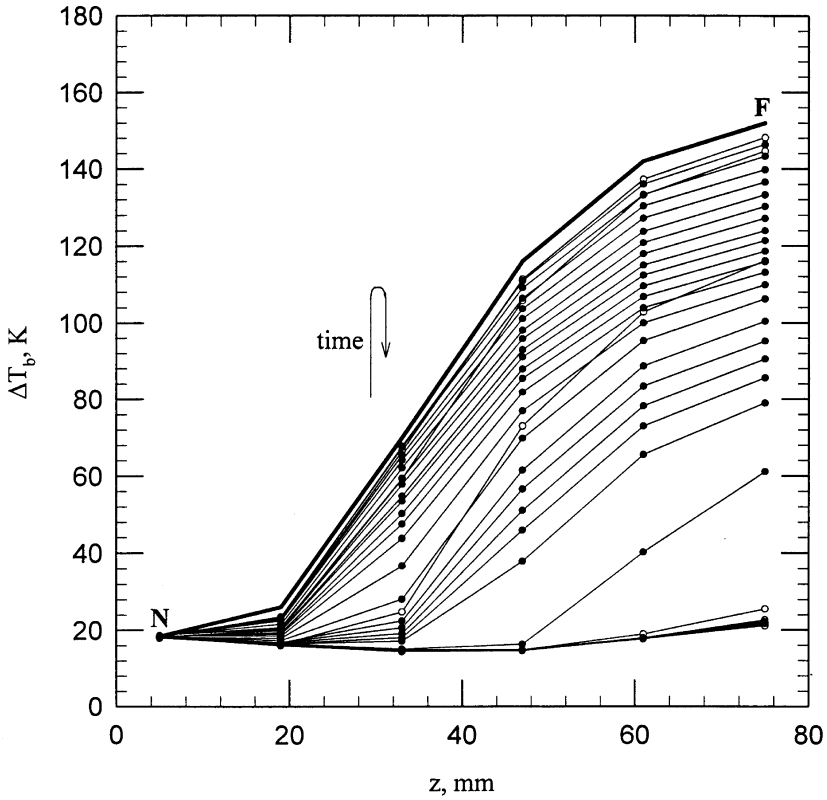


Fig. 4. (a) Time evolution of extrapolated, axial surface temperature distribution: time interval is 20 s; $V_1$, $V_2$, $V_3 = 80$, 220, 60 V respectively. Methanol: flow rate 20 km m$^{-2}$ s$^{-1}$, saturated liquid. Bold curve NF: coexisting curve with neutral stability. Open symbols: temperature increasing phase; closed symbols: temperature decreasing phase.

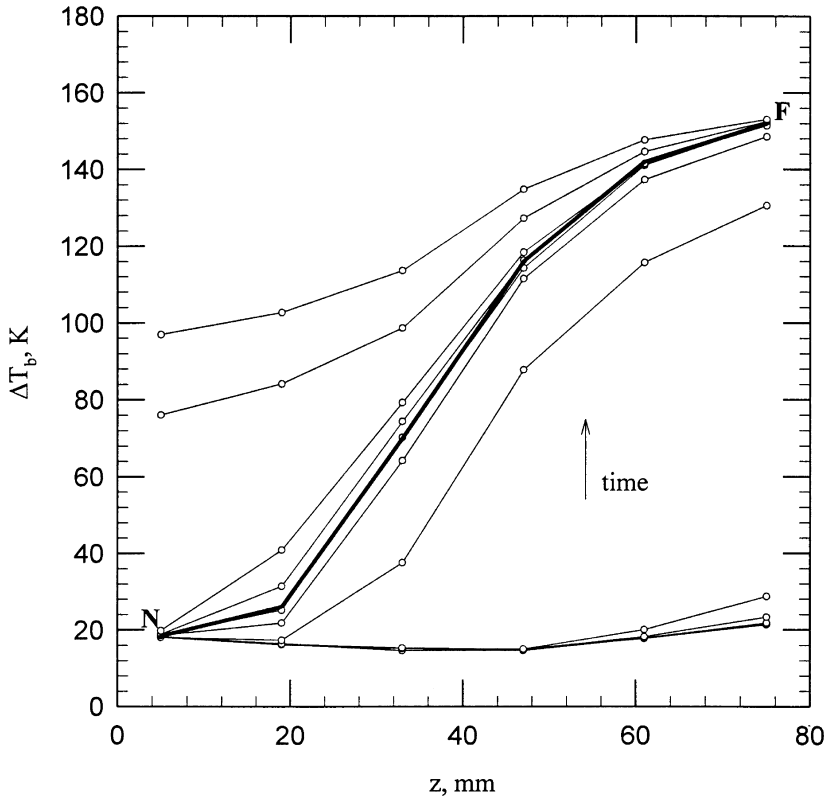


Fig. 4. (b) Time evolution of extrapolated, axial surface temperature distribution: time interval is 20 s; $V_1$, $V_2$, $V_3$ = 80, 220, 80 V respectively. Methanol: flow rate 20 kg m$^{-2}$ s$^{-1}$, saturated liquid. Bold curve NF: coexisting curve with neutral stability. Temperature: increasing phase only. Fig. 5: photographs of boiling at NF condition.

Table 1
$q_N$ and $q_F$ data

| | $\Delta T_{sub}$ = 0 K | | $\Delta T_{sub}$ = 10 K | | $\Delta T_{sub}$ = 20 K | |
|---|---|---|---|---|---|---|
| | $q_N$ | $q_F$ | $q_N$ | $q_F$ | $q_N$ | $q_F$ |
| $P$ = 760 mmHg | 0.40 | 0.15 | 0.55 | 0.14 | 0.95 | 0.13 |
| $Q$ = 12 kg m$^{-2}$ s$^{-1}$ | 0.35 | 0.19 | 0.35 | 0.30 | 0.84 | 0.20 |
| | 0.30 | 0.21 | | | | |
| $P$ = 760 mmHg | 0.48 | 0.143 | 0.70 | 0.10 | 1.0 | 0.15 |
| $Q$ = 20 kg m$^{-2}$ s$^{-1}$ | 0.40 | 0.17 | 0.68 | 0.21 | 0.80 | 0.61 |
| | 0.32 | 0.238 | 0.58 | 0.31 | | |
| | $P$ = 660 mmHg | | $P$ = 560 mmHg | | | |
| | $q_N$ | $q_F$ | $q_N$ | $q_F$ | | |
| $Q$ = 20 kg m$^{-2}$ s$^{-1}$ | 0.6 | 0.12 | 0.64 | 0.10 | | |
| $\Delta T_{sub}$ = 0 K | 0.35 | 0.25 | 0.44 | 0.21 | | |
| | 0.28 | 0.28 | 0.35 | 0.27 | | |

The heat fluxes are in MW m$^{-2}$.

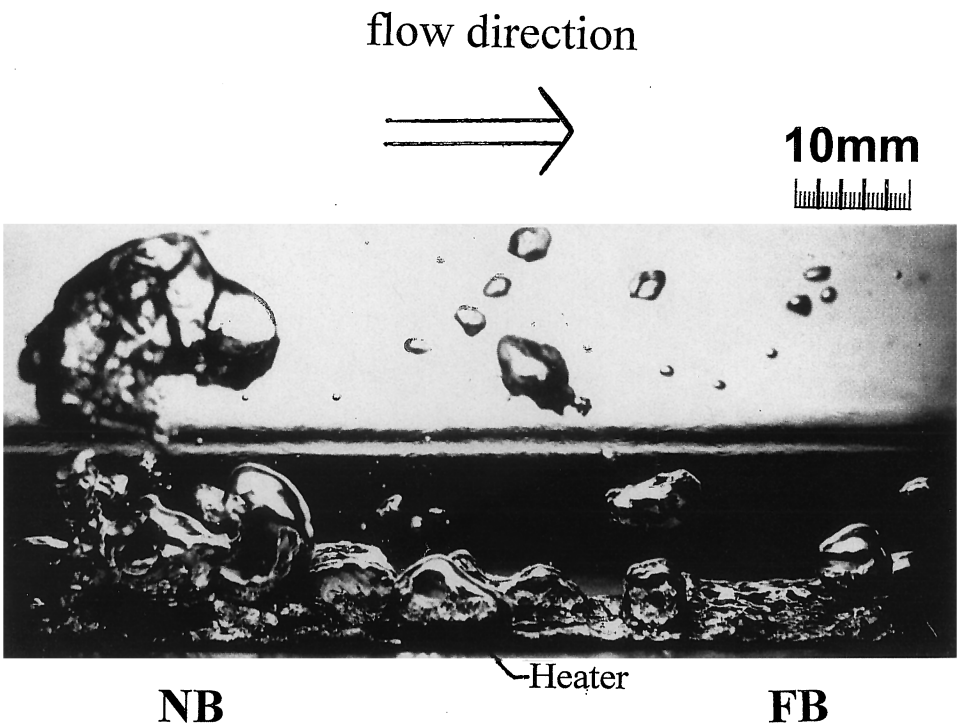


Fig. 5. Photograph of NF curve in Figs 4(a) and 4(b). NB: nucleate boiling; FB: film boiling.

direct experimental evidence for the existence of equilibrium heat flux on an indirectly conductive heating surface. The relative stability between different boiling systems can therefore be compared on the $q_C$ value. A higher $q_C$ denotes more stable nucleate boiling and less chance of burnout.

To provide further physical insights into this nonuniformly heated boiling process, we have solved the two-dimensional heat conduction equation via a commercial finite element solver, the PDEase v 2.4.4 (SPDE Inc., USA). Figure 9 depicts the computational domain. The scales of the computational domain are the same as those of the test block and heating assembly for the present experimental setup. The boundary conditions at the bottom surface show that the inflow heat flux is $q_N$ and $q_F$, respectively. (The left-hand block represents the B1–B3, while the right-hand block represents B4–B6.) The top boundary condition assumes that the heat conduction heat flux normal to the upper surface is equal to that dissipated by boiling heat transfer with a coefficient of $h_B$ (which is obtained from the average boiling curve data). A nonuniform temperature distribution is employed as the initial condition, while the steady-state solution is solved by iteration. The maximum relative error is set at $10^{-3}$. Typical job execution time is approximately 5 min on an IBM Pentium Pro personal computer, equipped with 16 Mb RAM and a 1 Gb hard disk.

Three distinct steady-state temperature distributions can be obtained: all surfaces in nucleate boiling mode, all in film boiling mode, and the coexisting boiling mode. By varying the bottom heat fluxes, the steady-state coexisting boiling mode is reached. Figure 10 illustrates typical numerical results for the coexisting mode, steady-state temperature distribution and the heat flux fields under various bottom heat fluxes $q_N$ and $q_F$. Notably, in Fig. 10(a), where $q_N > q_F$, the isothermal lines distort in accordance with the axial heat conduction through the bridge section. However, the region influenced by axial heat conduction is not large; most of the isothermal lines in both blocks are nearly parallel to the bottom. In contrast, in Fig. 10(c) where $q_N < q_F$, the isothermal lines and the heat flux distribution within the left-hand block are markedly distorted. Most of the left-hand block is influenced by the strong heat conduction from the right-hand block. Actually, in some parts of the left-hand block, the reversal of heat flux (the heat flows downwards rather than upwards) is noted. In such a case, a rather low $q_N$ is achieved. In Fig. 10(b), where $q_N$ is close to $q_F$, the temperature distributions in both blocks are similar. The heat fluxes through axial conduction have influenced the regions close to the bridge section. However, they do not affect the heat fluxes at both ends. At the two ends ($X = \pm 0.04$), the bottom heat flux is equal to the surface boiling heat flux $q_N$ and $q_F$.

The calculated $q_N$ and $q_F$ data are depicted by the open symbols in Fig. 8, from which we can note that the

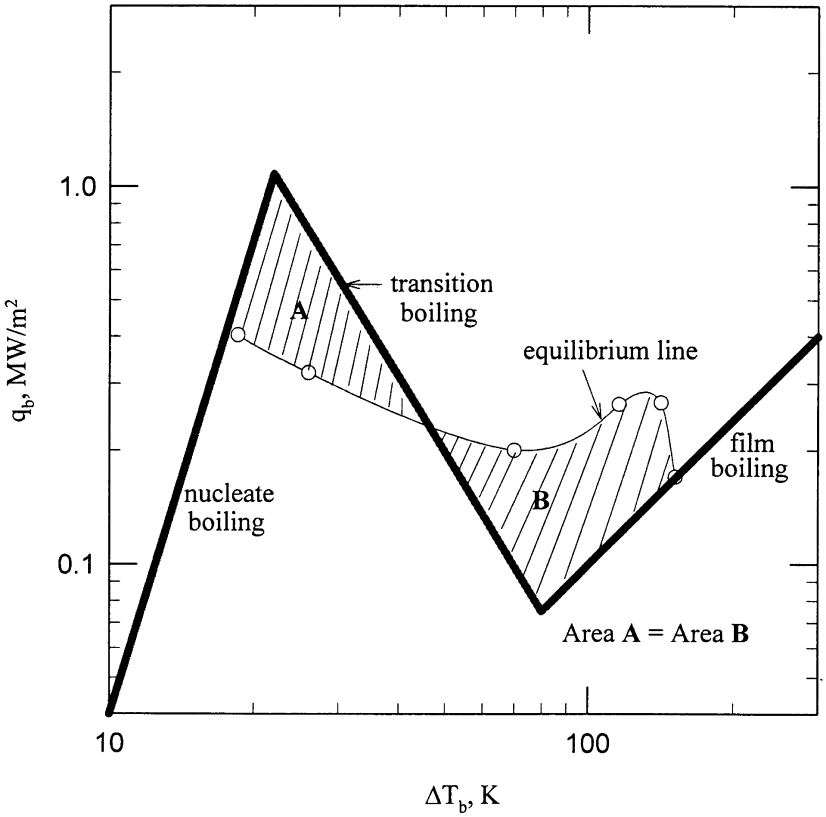


Fig. 6. Curve NF and boiling curves for Fig. 5.

agreement between simulation and experiment is acceptable. As a result, the $q_C$ data can be obtained both from experimental data extrapolation and numerical simulation.

Figure 11 depicts the extrapolated experimental $q_C$ data under various conditions. As expected, a higher mass flow rate and liquid subcooling will lead to a higher $q_C$, a more stable nucleate boiling mode. More precisely, since the $q_C$ for $Q = 20$ kg m$^{-2}$ s$^{-1}$ and $\Delta T_{sub} = 10$ K is similar to that for $Q = 12$ kg m$^{-2}$ s$^{-1}$ and $\Delta T_{sub} = 20$ K, their stability characteristics are considered to be similar also. However, the slight decrease in $q_C$ as the system pressure decreases denotes a less stable nucleate boiling at elevated system pressure. This is somewhat surprising since at first sight the nucleate boiling should be more efficient as the system pressure goes up. It can be explained as the $q_C$ value being actually a relative estimate for the stability characteristics of nucleate and film boiling on the same heating surface. A higher system pressure would give a more efficient nucleate boiling, however, the film boiling mode is enhanced also. According to the present experimental data, their relative stability does not change much within the experimental range. The greater $q_C$ under subcooled conditions or with a high cross flow reveals relatively more stable nucleate boiling.

## 4. Conclusions

Flow boiling of methanol over a nonuniformly heated surface is investigated under atmospheric and subatmospheric pressures. The equal-area criterion is employed as a basis of data interpretation. Results in this study, reveal that a decrease in liquid subcooling and/or system pressure, or an increase in nucleate boiling bottom heat flux tends to weaken the relative stability of the nucleate boiling. The liquid flow rate has little influence within the experimental range, however, the nucleate boiling mode on the leading portion of the heating surface along the flow direction would be more stable. The 'equilibrium heat flux' proposed by Kovalev [4] is, for the first time, proven to exist on an indirectly conducting heated surface, which can serve as a direct comparison between stability characteristics of different boiling systems. The relative stability of nucleate boiling increases as liquid subcooling or mass flowrate increases, and is not strongly

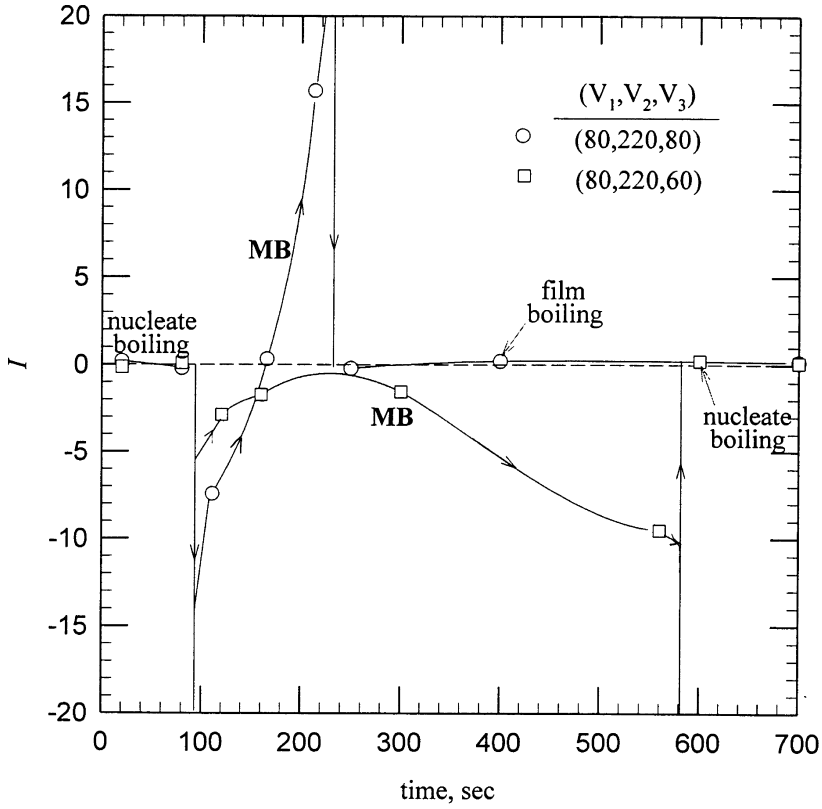


Fig. 7. *I* values for boiling sequences in Figs 2 and 3.

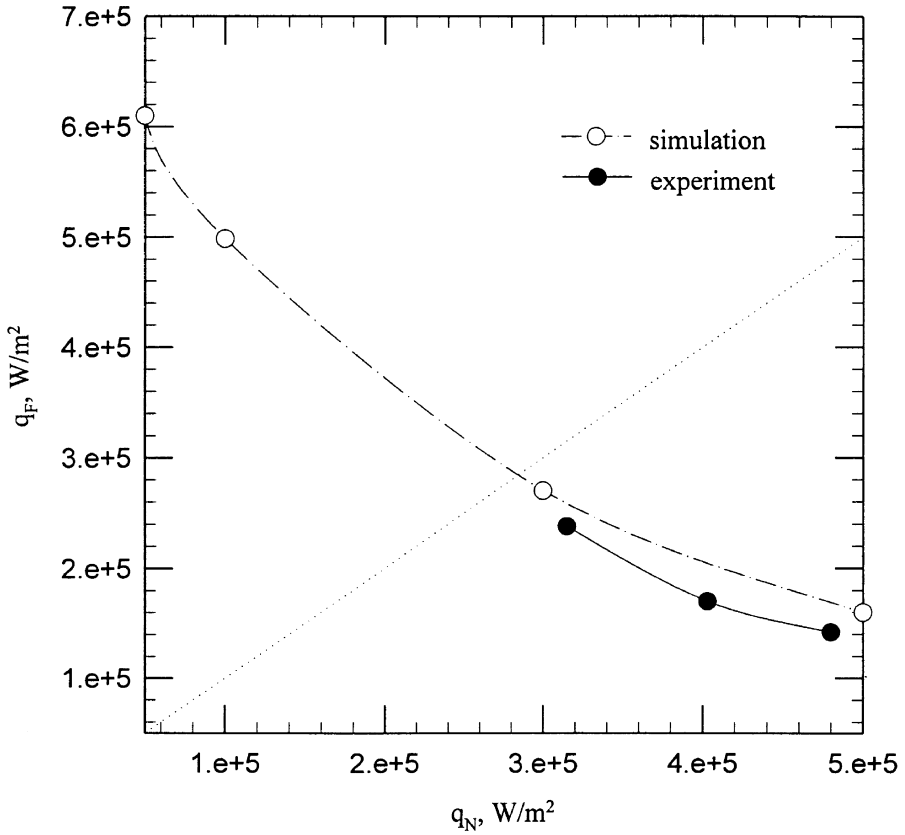


Fig. 8. $q_N$ vs $q_F$ data for $P = 760$ mmHg, $Q = 20$ kg m$^{-2}$ s$^{-1}$, $\Delta T_{sub} = 0$ K. Closed symbols: experiments; open symbols: simulation results.

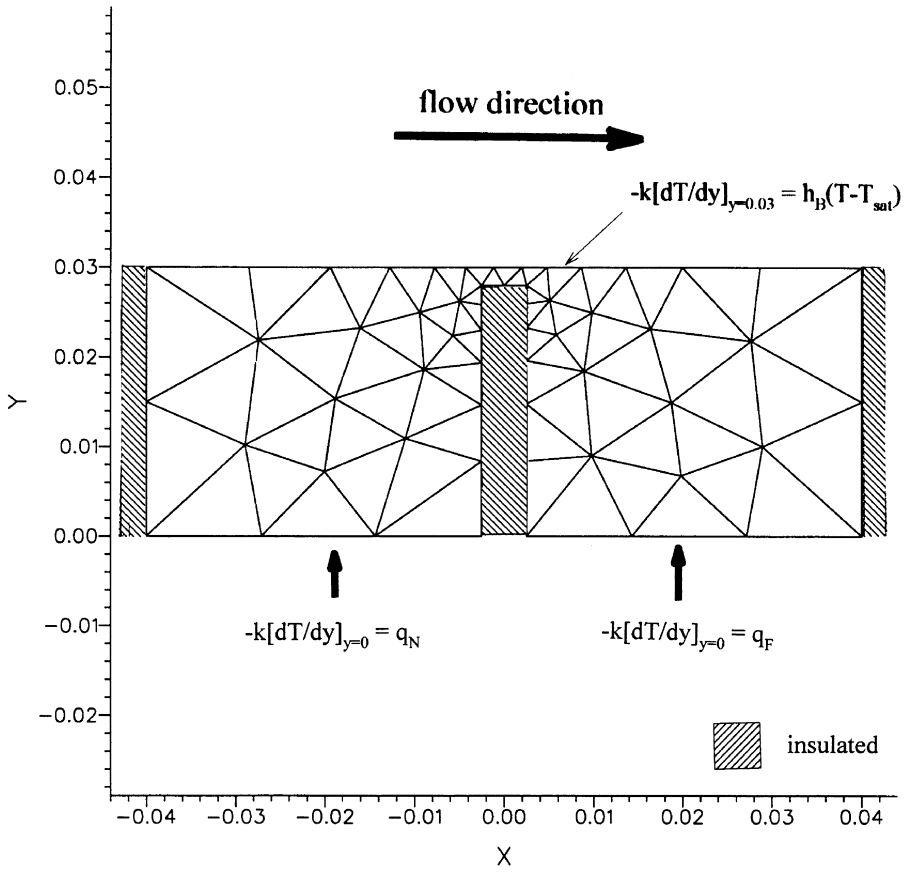


Fig. 9. Computational domain in simulation works.

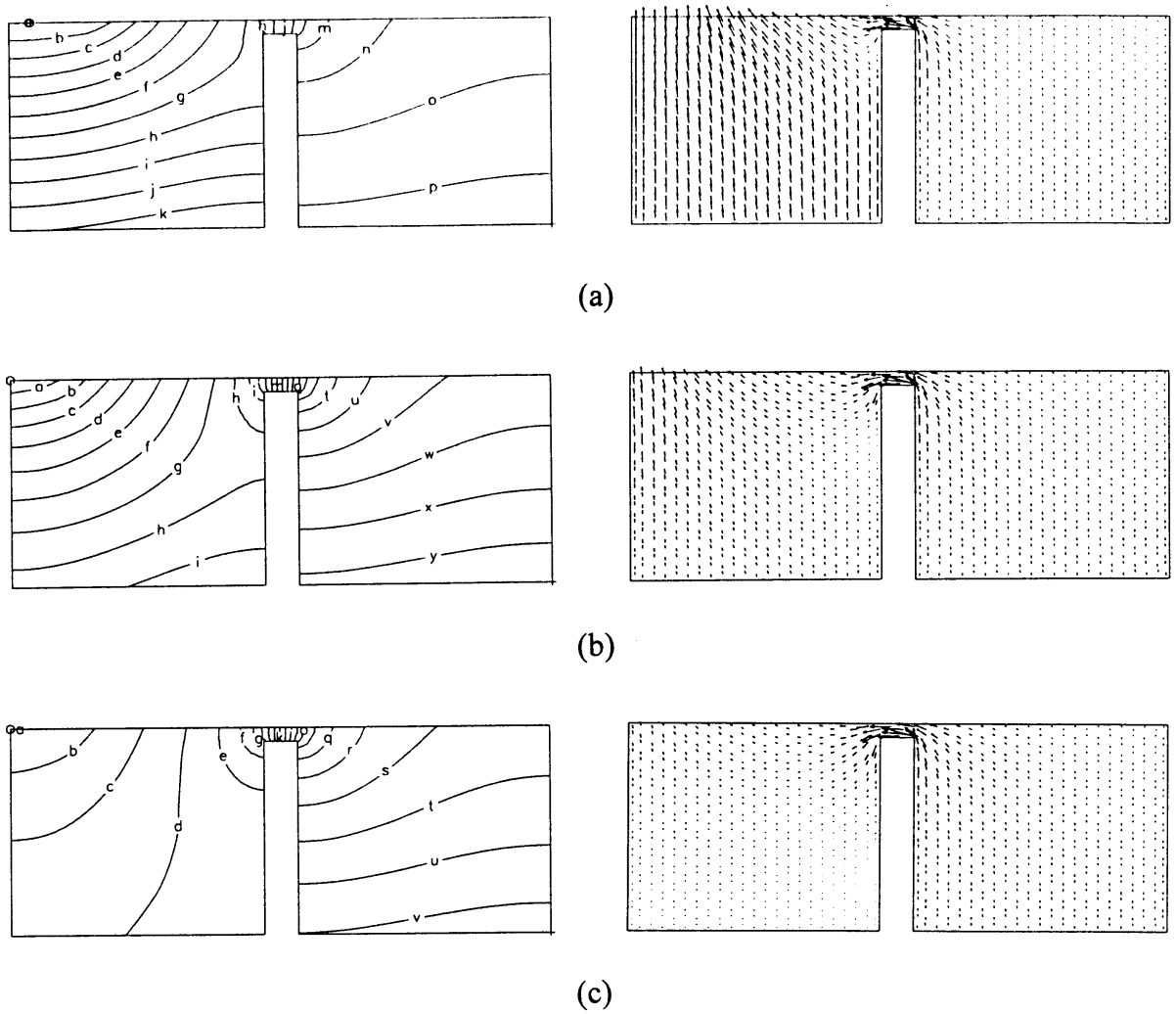


Fig. 10. Isothermal lines and heat flux plots: (a) a = 85°C, p = 160°C; (b) a = 90°C, y = 210°C; (c) a = 90°C, v = 300°C.

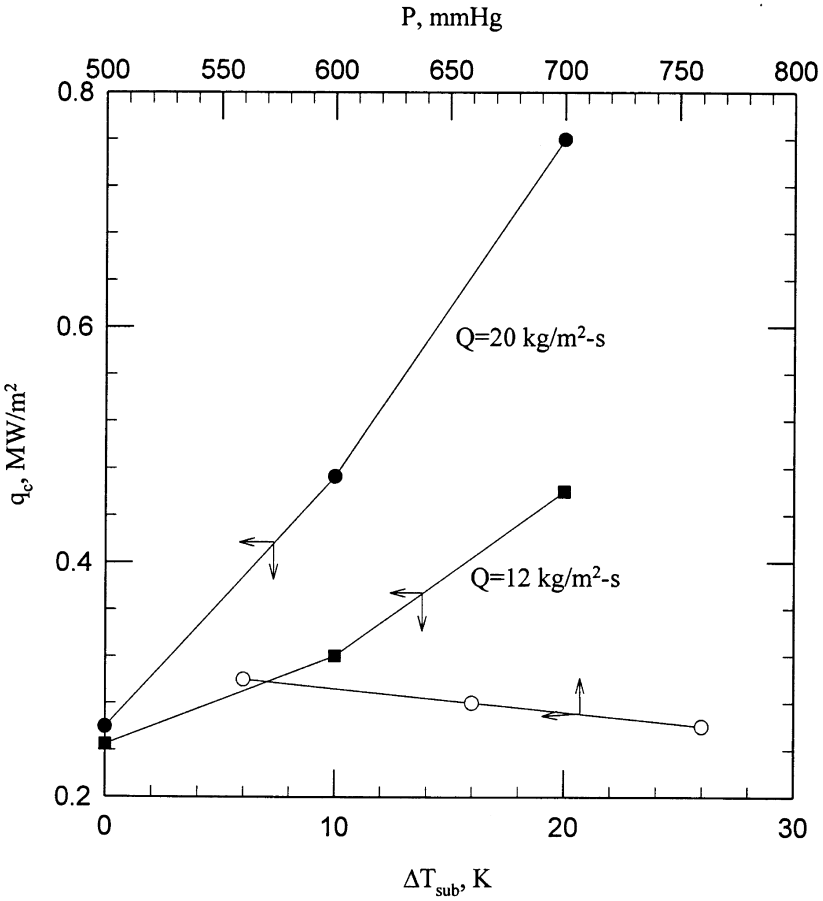


Fig. 11. $q_C$ vs $\Delta T_{sub}$ and $P$.

influenced by system pressure. Results from numerical analysis agree well with the experimental data.

## References


[1] Lu SM, Lee DJ. Effects of heater and heating methods on pool boiling. AIChE J 1989;35:1742–44.

[2] Lu SM, Lee DJ. The effects of heating methods on pool boiling. Int J Heat Mass Transfer 1991;34:127–34.

[3] Lee DJ, Lu SM. Two-mode boiling on a horizontal heating wire. AIChE J 1992;38:1115–28.

[4] Kovalev SA. An investigation of minimum heat fluxes in pool boiling. Int J Heat Mass Transfer 1966;9:1219–26.

[5] Zhukov SA, Barelko VV. Nonuniform steady states of the boiling process in the transition region between the nucleate and film regimes. Int J Heat Mass Transfer 1983;26:1121–30.

[6] Zhukov SA, Barelko VV, Merzhanov AG. Wave processes on heat generating surfaces in pool boiling. Int J Heat Mass Transfer 1980;24:47–55.

[7] Zhukov SA, Bokova LF, Barelko VV. Certain aspects of autowave transitions from nucleate to film boiling regimes with a cylindrical heat generating element inclined from a horizontal position. Int J Heat Mass Transfer 1983;26:269–75.

[8] Tachibana F, Akiyama M, Kawamura H. Non-hydrodynamic aspects of pool boiling burnout. J Nucl Sci Tech 1967;4:121–30.

[9] Lee DJ. Effects of heater properties, heating methods and liquid subcooling on pool boiling. Ph.D. Dissertation. National Taiwan University, Taipei, 1989.

[10] Lin WW, Lee DJ. Relative stability between nucleate and film boiling on a nonuniformly heated flat surface. ASME J Heat Transfer 1997;119:326–31.

[11] Kline SJ, McClintock FA. Description of uncertainties in single sample experiments. Mech Eng 1953;75:3–8.

[12] Passos JC, Gentile D. An experimental investigation of transition boiling in subcooled Freon-113 forced flow. ASME Journal of Heat Transfer 1991;113:459–62.

[13] Blum J, Marquardt W. Stability of boiling systems. Int J Heat Mass Transfer 1996;39:3021–33.